Article

A broadband signal recycling scheme for saturating the quantum limit from optical losses

Teng Zhang, Joe Bentley and Haixing Miao

[1] School of Physics and Astronomy, and Institute of Gravitational Wave Astronomy, University of Birmingham, Edgbaston, Birmingham B15 2TT, United Kingdom

* Correspondence: tzhang@star.sr.bham.ac.uk

Abstract: Quantum noise limits the sensitivity of laser interferometric gravitational-wave detectors. Given the state-of-the-art optics, the optical losses define the lower bound of best possible quantum-limited detector sensitivity. In this work, we come up with the configuration which allows to saturate this lower bound by converting the signal recycling cavity to be a broadband signal amplifier using an active optomechanical filter. We will show the difference and advantage of such a broadband signal recycling scheme compared with the previous white-light-cavity scheme using the optomechanical filter in [Phys.Rev.Lett.115.211104 (2015)]. The drawback is that the new scheme is more susceptible to the thermal noise of the mechanical oscillator. To suppress the radiation pressure noise which rises along with the signal amplification, squeezing with input/output filter cavities and heavier test mass are used in this work.

Keywords: quantum loss limit; broadband signal recycling; optomechanical filter cavity

1. Introduction

The ground-based laser interferometric gravitational-wave detectors operate at a frequency band from several Hz to several kHz. The quantum noise is one of the most important noises which limits the detector sensitivity nearly over the entire frequency band. To enhance the quantum-limited sensitivity, the first limit we encounter is the *Standard Quantum limit*, which is related to the *Heisenberg uncertainty principle* of the optical quadratures [1]. It is defined as the minimal sum of the quantum shot noise and radiation pressure noise (when uncorrelated) at each frequency, given different optical power. However, it does not describe the best achievable quantum-limited sensitivity. The next limit is the *Quantum Cramér-Rao Bound* [2], or the so called energetic/fundamental quantum limit [3–5], which shows the minimum quantum uncertainty is determined by the quantum energy fluctuation. This bound can be infinitely reduced by improving the energy fluctuation inside the arm cavities, *e.g.* enhancing the optical power and using quantum squeezing (anti-squeezing). It was recently realised that the practical lower bound of the quantum-limited sensitivity comes from the optical loss induced quantum dissipation [6].

The optical losses are unavoidable in real detectors and can come from various sources, *e.g.*, absorption, scattering, and mode mismatch. Depending on the mechanism how the optical losses couple to the gravitational-wave signal channel, they can be classified into the internal loss, including the arm cavity loss $\epsilon_{\rm arm}$ and the signal recycling cavity (SRC) loss $\epsilon_{\rm SRC}$, and the external loss in the output chain $\epsilon_{\rm ext}$. The sensitivity limit due to these optical losses is given by [6]:

$$S_\epsilon = \frac{\hbar c^2}{4L^2\omega_0 P_{\rm arm}}\left[\epsilon_{\rm arm} + \frac{(\Omega^2+\gamma_{\rm arm}^2)T_{\rm ITM}}{4\gamma_{\rm arm}^2}\epsilon_{\rm SRC} + \frac{1}{4}T_{\rm SRC}\epsilon_{\rm ext}\right], \quad (1)$$

where ω_0 is the laser frequency, Ω is the angular frequency of gravitational wave signals, L is the arm length, $P_{\rm arm}$ is the arm cavity power, $T_{\rm ITM}$ is the input test mass (ITM) transmissivity, $\gamma_{\rm arm} = cT_{\rm ITM}/(4L)$ is the arm cavity bandwidth and $T_{\rm SRC}$ is the effective transmissivity of the signal recycling cavity (SRC) formed by ITM and the signal-recycling mirror (SRM). The arm cavity loss limited

Preprints (www.preprints.org) | NOT PEER-REVIEWED | Posted: 16 November 2020 doi:10.20944/preprints202011.0405.v1

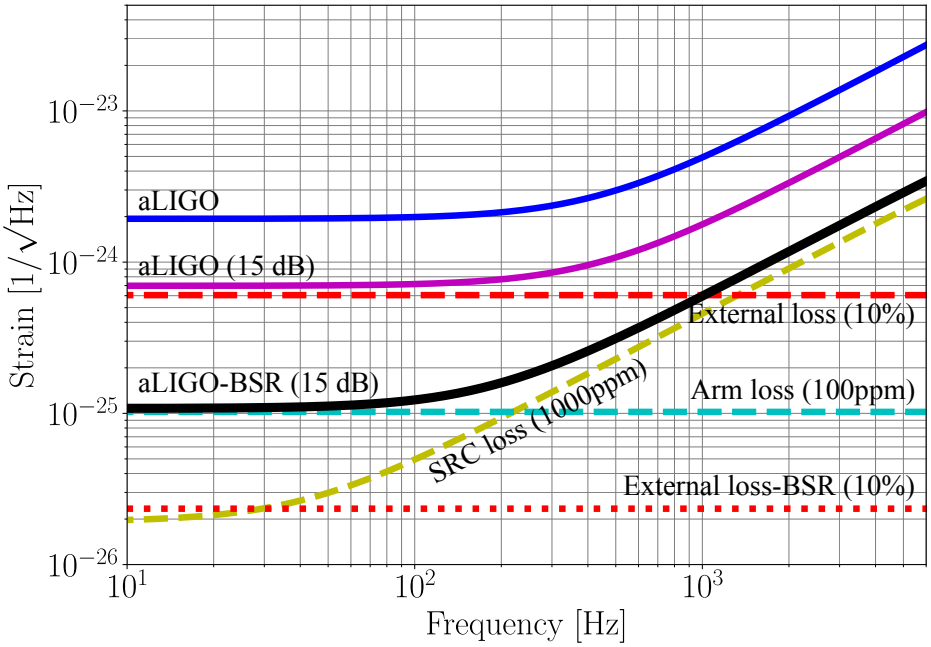

Figure 1. This figure shows the noise spectral densities of optical losses and the shot noise limited sensitivity with parameters from aLIGO configuration. We assumed 1000 ppm totally effective SRC loss, 100 ppm arm cavity loss and 10% external loss. The blue line illustrates the shot noise of aLIGO. The purple line is with 15 dB squeezing ($\sim$ 9 dB observed). The black line illustrates the resulting shot noise of the aLIGO configuration with the broadband signal recycling (BSR) scheme discussed in this work. It saturates the SRC loss introduced noise in high frequencies and external loss limit in low frequencies. The reduction of external loss limit from dash-red line to dot-red line comes from the utilisation of the broadband signal recycling scheme.

sensitivity is frequency independent, since the vacuum fluctuation from the loss mixes with the signals directly inside the arm cavity. In contrast, the SRC loss limited sensitivity rises at higher frequencies above the arm cavity bandwidth, due to a decrease of signal response of the arm cavity. It is independent of any optical modules inside the SRC. The external loss happens in the output chain of the interferometer, where there are unwanted effects including the mode mismatch at the output mode cleaner, and an imperfect quantum efficiency of the photodiode. The output loss effect can be modeled as the arm cavity loss after the reduction of $T_{\rm SRC}$, which depends on the SRC configuration and equals to 0.14 in advanced LIGO (aLIGO). Apparently, it also limits the observed squeezing level. For example, with 10% external loss, the observed squeezing cannot be more than 10 dB. Fig. 1 shows the result of optical-loss induced limits for aLIGO [7].

From Eq. (1), we learn that at high frequencies, *i.e* $\Omega \gg \gamma_{\rm arm}$, the best achievable quantum sensitivity is limited by the SRC loss with spectral density

$$\frac{\hbar\Omega^2}{\omega_0 P_{\rm arm} T_{\rm ITM}} \epsilon_{\rm SRC}\,, \tag{2}$$

which turns out to be independent of the arm length. It is then exciting and crucial to explore the way of saturating the high frequency quantum limit, which will give the maximal astrophysical outcome, in particular on neutron star physics [8,9]. As shown in Fig. 1, the sensitivity of aLIGO with 10 dB observed squeezing is still one order of magnitude worse than the SRC loss limit with $\epsilon_{\rm SRC} = 1000$ ppm in the frequency range of 1-5 kHz.

Up to now, the proposed quantum techniques can be categorized into the following two classes: (1) noise suppression/cancellation schemes; (2) signal amplification schemes. The strategies that allow us to overcome the standard quantum limit are known as *Quantum-nondemolition techniques* [10,

Preprints (www.preprints.org) | NOT PEER-REVIEWED | Posted: 16 November 2020 doi:10.20944/preprints202011.0405.v1

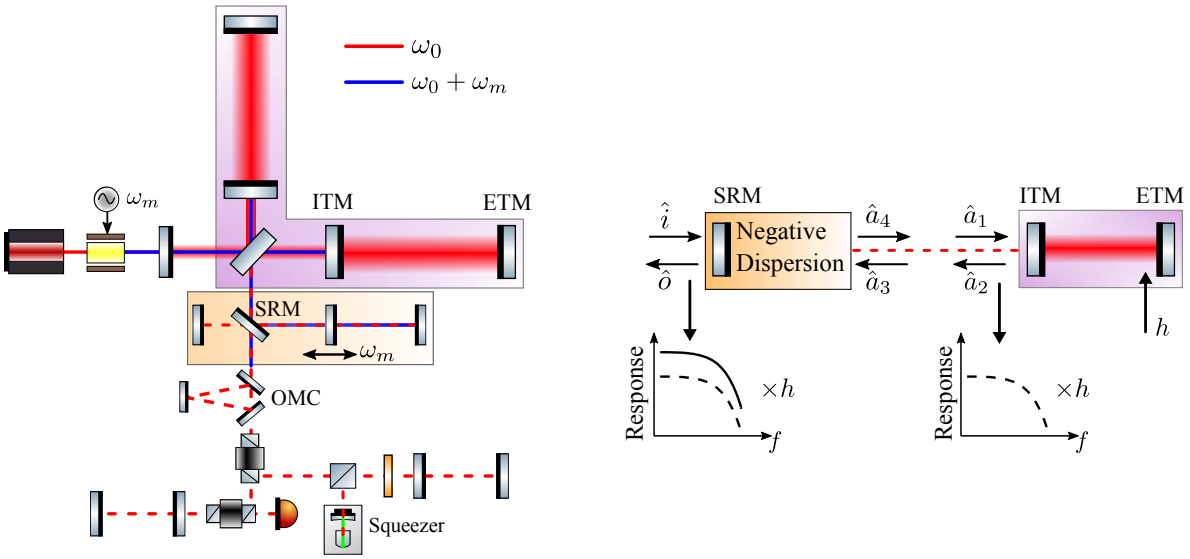

Figure 2. Left: Gravitational wave detector with the proposed broadband signal recycling scheme and input/output filter cavities. The carrier laser is at ω_0 (red). The optomechanical filter cavity is pumped with a laser at $\omega_0 + \omega_m$ (blue), which comes from the modulation of the input carrier and travels to the dark port due to the Schnupp asymmetry. The mechanical frequency of the oscillator of the optomechanical filter cavity is ω_m. The blue beam is filtered with an output mode cleaner (OMC). The input and output filter cavity are placed for frequency dependent squeezing and variational readout. Right: Simplified schematic of the broadband signal recycling scheme. Inside the SRC, the phase of sidebands reflecting from the arm cavity is compensated by the negative dispersion, thus the SRC is on resonance at all frequencies. The SRC is converted to be an amplifier for the signals coming out from the arm cavity with a gain of $1/\sqrt{T_{\rm SRM}}$.

11], for example, frequency dependent squeezing and variational readout [12], which are also used in this work. Based on the understanding from the optical loss limit, despite utilizing internal or external squeezing [13–16] for the purpose of noise suppression, the observed squeezing level has an unsurpassed bound due to external loss. The signal enhancement scheme can complement the squeezing for achieving the quantum limit from optical losses. The most well-known signal amplification technique, which has already been implemented in the second-generation detectors, is the signal-recycling cavity. Obviously, both the high frequency and low frequency sensitivity can be improved under tuned *Resonate sideband extraction* mode. However, this comes with a price of sacrificing the peak sensitivity at intermediate frequencies. Such a trade-off is the so called *peak sensitivity-bandwidth product*. It is due to the accumulation of the phase of the sidebands traveling inside the cavity (positive dispersion), which leads to the destructive interference of sidebands with frequencies larger than the cavity bandwidth. Another recent work on high-frequency detector design uses the coupled cavity resonance from the the coupling of the arm cavity and the SRC in the *Resonate sidebands extraction* mode. This scheme gives rise to a narrow band dip in the noise spectrum at high frequencies [9,17]. In this scheme, such a coupled cavity resonance shows up when the sidebands resonate in the SRC after a round trip reflecting off from both arm cavities and the SRM. And similar to the arm cavity, the sidebands in the SRC can also only resonate in a narrow band due to the phase accumulation from both arm cavity and the free space. Equivalently, the identical resonance condition appears at DC frequency when the signal recycling cavity is tuned to the so called *signal recycling* mode.

One strategy to broaden up the bandwidth without sacrificing the peak sensitivity is to introduce negative dispersion to compensate the arm cavity round trip phase, $2\Omega L_{\rm arm}/c$, by means of white light cavities [18–20]. However, as it turns out, there is an imperfect phase compensation out of the

Preprints (www.preprints.org) | NOT PEER-REVIEWED | Posted: 16 November 2020 doi:10.20944/preprints202011.0405.v1

first order linear dispersion region, which eventually leads to a rapid decrease of sensitivity above a certain frequency.

The coupled SRC and arm cavity cavity design and white light cavity idea are heuristic. In our proposed scheme proposed to saturate the quantum loss limit in this work, a frequency dependent coupled cavity resonance is realised. We name it as the broadband signal recycling (BSR) scheme.

2. Design concept and quantum noise

The scheme we propose in this work is shown in Fig. 2. Inside the SRC, an optomechanical filter cavity which provides the negative dispersion is placed for canceling the phase of the sidebands gained reflecting from the arm cavity. The length of the SRC should be short enough so that the propagation phase of sidebands can be neglected. The optomechanical filter cavity is pumped with the laser at frequency $\omega_0 + \omega_m$, which is generated from the modulation on the input carrier light at frequency ω_0. A Schnupp asymmetry allows the pump laser to transmit to the dark port. It is worthwhile to note the difference compared with the previous scheme in [19]. In that configuration, an addition mirror so-called iSRM is introduced to achieve an impedance match with the ITM of the arm cavity, which effectively removes the ITM for the sidebands. The negative dispersion is then compensating the positive dispersion within the arm cavity. However, as we mentioned above, the compensation is not naturally perfect at higher frequencies. Here we show the iSRM (extra complexity) is not required and we can follow the loss limit in high frequency because of a naturally exact phase compensation in ideal case.

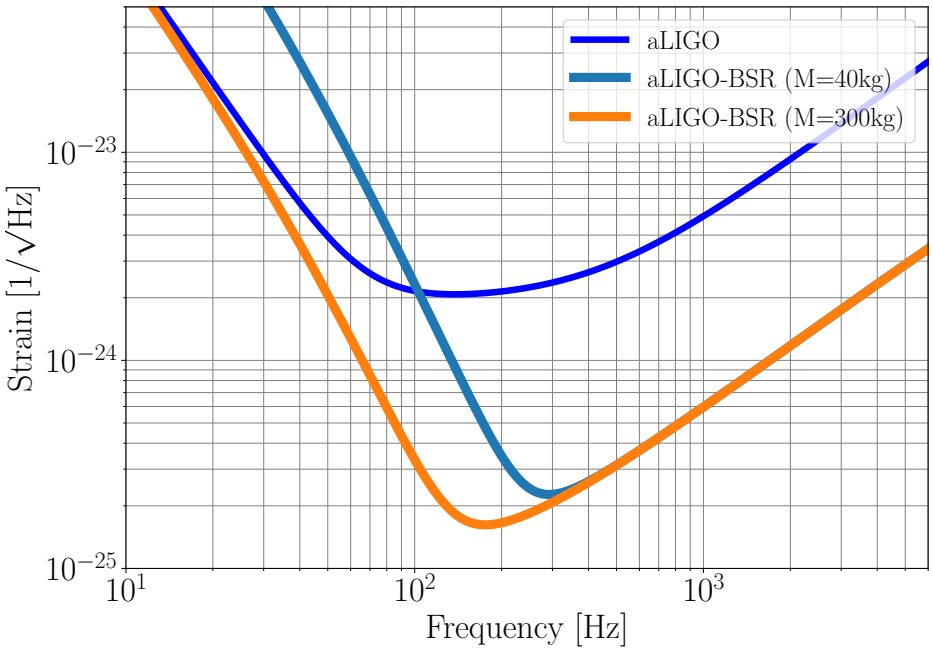

Figure 3. This figure shows the quantum noise spectral densities of aLIGO and two BSR configurations with test mass 40 kg and 300 kg, respectively. 15 dB squeezing and both input/output filter cavity are used for frequency dependent squeezing and variational readout. The optical losses are the same as in Fig. 1

.

In Fig. 2, the optical input/output relation between the output field from the arm cavity $\hat{a}_2$ and the input field $\hat{a}_1$ can be derived as

$$\hat{a}_2 \approx \frac{\gamma_{\rm arm} + i\Omega}{\gamma_{\rm arm} - i\Omega}\hat{a}_1 = e^{i\beta}\hat{a}_1\,, \tag{3}$$

Preprints (www.preprints.org) | NOT PEER-REVIEWED | Posted: 16 November 2020 doi:10.20944/preprints202011.0405.v1

where $\beta = 2\text{atan}\frac{\Omega}{\gamma_{\text{arm}}}$ is the phase gained by the sidebands with frequency Ω reflecting from the arm cavity. In order to compensate this frequency dependent phase inside the SRC and convert the SRC to be a signal amplifier, we need to introduce a phase with the negative dispersion. As it turns out, this can be exactly provided by an optomechanical filter in the so-called resolved-sideband regime, *i.e.* $\omega_m \gg \gamma_f \gg \Omega$, where ω_m is the mechanical resonate frequency, γ_f is the filter cavity bandwidth. When the mechanical damping rate, γ_m is much smaller than the negative mechanical damping rate due to the optomechanical interaction, γ_{opt}, the optomechanical filter cavity gives the following open-loop transfer function [19]

$$\hat{a}_{out} \approx -\frac{\gamma_{\text{opt}} - i\Omega}{\gamma_{\text{opt}} + i\Omega}\hat{a}_{in} = e^{i\alpha}\hat{a}_{in}\,, \tag{4}$$

where $\gamma_{\text{opt}} = P\omega_0/(m\omega_m c L_f \gamma_f)$ and $\gamma_m = \omega_m/Q_m$, m is the mass of the mechanical oscillator, Q_m is the quality factor, and P is the power in the optomechanical filter at the pumping laser frequency $\omega_0 + \omega_m$. When

$$\gamma_{\text{opt}} = \gamma_{\text{arm}}\,, \tag{5}$$

there is an exact cancellation of α and β up to a frequency-independent constant: $\alpha + \beta = \pi$. With the signal recycling mirror tuned to give another constant π phase shift, the SRC is on resonance at all frequencies. As it turn out, in the output filed $\hat{o}$, the signals in $\hat{a}_2$ will be amplified with constant gain $1/\sqrt{T_{\text{SRM}}}$ with the SRC layout in the left part of Fig. 2, where T_{SRM} is the power transmissivity of the SRM. The effective transmissivity of the SRC is

$$T_{\text{SRC}} = \frac{T_{\text{ITM}}T_{\text{SRM}}}{(1+\sqrt{R_{\text{ITM}}R_{\text{SRM}}})^2}\,, \tag{6}$$

where R_{ITM}, R_{SRM} is the power reflectivity of the ITM and SRM. In the optomechanical filter cavity, the thermal noise effect of the mechanical oscillator can be modelled as an effective optical loss [8],

$$\epsilon_{eff} = \frac{4k_B}{\hbar\gamma_{opt}}\frac{T_{env}}{Q_m}\,, \tag{7}$$

where k_B is the Boltzmann constant, T_{env} is the environmental temperature. It act as an effective SRC loss. In our case, to assume an effective SRC loss contribution ~ 200 ppm, the ratio T_{env}/Q_m has to be $\sim 10^{-13}$. This gives a more stringent requirement, which is the drawback of the BSR scheme compared with the scheme in [19]. This is because the required of γ_{opt} is smaller compared with that in [19], which equals to c/L.

After taking into account frequency dependent squeezing and variational readout as show in Fig. 2, the spectral density of the detector can be calculated as the sum of [21]

$$S = \frac{h_{\text{SQL}}^2}{2}\left[\frac{e^{-2r}+\epsilon_{\text{ext}}}{\mathcal{K}} + \frac{\epsilon_{\text{ext}}}{1+\epsilon_{\text{ext}}e^{2r}}\mathcal{K}\right]\,, \tag{8}$$

and the SRC and arm cavity loss contribution, where $e^{-2r} \approx 0.03$ represents ~ 15 dB squeezing. $\mathcal{K}$ is the famous Kimble factor and h_{SQL} is the standard quantum limit,

$$\mathcal{K} = \frac{16\omega_0 P_{\text{arm}}\gamma_{\text{arm}}T_{\text{SRM}}}{McL\Omega^2(\gamma_{\text{arm}}^2+\Omega^2)}\,, \quad h_{\text{SQL}} = \sqrt{\frac{8\hbar}{(M\Omega^2L^2)}}\,. \tag{9}$$

Here M is the mass of the detector test mass. We adopt $T_{\text{SRM}} = 0.005$ and $T_{\text{ITM}} = 0.014$, thus $T_{\text{SRC}} = 0.00002$. The arm cavity power P_{arm} is 800kW and arm length L is 4 km. The resulting shot-noise-limited sensitivity which corresponds to the sum of the first term in Eq. 8 and the loss limits is shown in Fig. 1. As we can observe the shot-noise-limited sensitivity of the BSR scheme saturate

the arm cavity loss limit at low frequencies and the SRC loss limit in high frequencies. Including the radiation pressure noise, the detector sensitivities are shown in Fig. 3, in which heavier 300 kg test masses are also considered.

3. Summary and outlook

In this work, we show one scheme that can saturate the optical loss limited sensitivity. A radiation pressure limited optomechanical filter inside the SRC provides a proper negative dispersion that cancels the frequency-dependent phase of the signal sidebands when reflecting from the arm cavity. It allows the simultaneous resonance of different sidebands in the SRC, which can be viewed as a frequency dependent coupled-cavity resonance. Instead of suppressing the noises which will be limited by losses, the signals are amplified in this scheme. The amplification gain is $1/\sqrt{T_{\rm SRM}}$ in amplitude. Note that the radiation pressure noise will also be amplified by the same amount, and the BSR scheme alone cannot overcome the standard quantum limit. The broadband signal recycling scheme realise the recycling for broadband signals similar to the power recycling for the carrier light. For future detectors beyond the aLIGO, using high gain of BSR cavity provide a new approach to reducing the shot noise, complementary to squeezing and increasing the power. A balance between the laser power and signal recycling gain may provide an easier access to cryogenic techniques for reducing classical noises, *e.g.* cryogenic temperature which are proposed for LIGO Voyager [22], the Einstein Telescope low-frequency detector [23,24], and Cosmic Explorer phase II [25].

Acknowledgements — T. Z., J.B. and H. M. acknowledge the support of the Institute for Gravitational Wave Astronomy at University of Birmingham. H. M. is supported by UK STFC Ernest Rutherford Fellowship (Grant No. ST/M005844/11).

1. Braginsky, V.B.; Khalili, F.Y.; Thorne, K.S. *Quantum Measurement*; Cambridge University Press, 1992. doi:10.1017/CBO9780511622748.
2. Helstrom, C. Minimum mean-squared error of estimates in quantum statistics. *Physics Letters A* **1967**, *25*, 101 – 102. doi:https://doi.org/10.1016/0375-9601(67)90366-0.
3. Braginsky, V.B.; Gorodetsky, M.L.; Khalili, F.Y.; Thorne, K.S. Energetic quantum limit in large-scale interferometers. *AIP Conference Proceedings* **2000**, *523*, 180–190. doi:10.1063/1.1291855.
4. Tsang, M.; Wiseman, H.M.; Caves, C.M. Fundamental Quantum Limit to Waveform Estimation. *Phys. Rev. Lett.* **2011**, *106*, 090401. doi:10.1103/PhysRevLett.106.090401.
5. Miao, H.; Adhikari, R.X.; Ma, Y.; Pang, B.; Chen, Y. Towards the Fundamental Quantum Limit of Linear Measurements of Classical Signals. *Phys. Rev. Lett.* **2017**, *119*, 050801. doi:10.1103/PhysRevLett.119.050801.
6. Miao, H.; Smith, N.D.; Evans, M. Quantum Limit for Laser Interferometric Gravitational-Wave Detectors from Optical Dissipation. *Phys. Rev. X* **2019**, *9*, 011053. doi:10.1103/PhysRevX.9.011053.
7. Aasi, J.; Abbott, B.P.; Abbott, R.; Abbott, T.; others. Advanced LIGO. *Classical and Quantum Gravity* **2015**, *32*, 074001. doi:10.1088/0264-9381/32/7/074001.
8. Miao, H.; Yang, H.; Martynov, D. Towards the design of gravitational-wave detectors for probing neutron-star physics. *Phys. Rev. D* **2018**, *98*, 044044. doi:10.1103/PhysRevD.98.044044.
9. Martynov, D.; Miao, H.; Yang, H.; Vivanco, F.H.; Thrane, E.; Smith, R.; Lasky, P.; East, W.E.; Adhikari, R.; Bauswein, A.; Brooks, A.; Chen, Y.; Corbitt, T.; Freise, A.; Grote, H.; Levin, Y.; Zhao, C.; Vecchio, A. Exploring the sensitivity of gravitational wave detectors to neutron star physics. *Phys. Rev. D* **2019**, *99*, 102004. doi:10.1103/PhysRevD.99.102004.
10. Braginsky, V.B.; Vorontsov, Y.I.; Thorne, K.S. Quantum Nondemolition Measurements. *Science* **1980**, *209*, 547–557. doi:10.1126/science.209.4456.547.
11. Chen, Y.; Danilishin, S.L.; Khalili, F.Y.; Müller-Ebhardt, H. QND measurements for future gravitational-wave detectors. *General Relativity and Gravitation* **2011**, *43*, 671–694. doi:10.1007/s10714-010-1060-y.

12. Kimble, H.J.; Levin, Y.; Matsko, A.B.; Thorne, K.S.; Vyatchanin, S.P. Conversion of conventional gravitational-wave interferometers into quantum nondemolition interferometers by modifying their input and/or output optics. *Phys. Rev. D* **2001**, *65*, 022002. doi:10.1103/PhysRevD.65.022002.
13. Adya, V.B.; Yap, M.J.; Töyrä, D.; McRae, T.G.; Altin, P.A.; Sarre, L.K.; Meijerink, M.; Kijbunchoo, N.; Slagmolen, B.J.J.; Ward, R.L.; McClelland, D.E. Quantum enhanced kHz gravitational wave detector with internal squeezing. *Classical and Quantum Gravity* **2020**, *37*, 07LT02. doi:10.1088/1361-6382/ab7615.
14. Korobko, M.; Kleybolte, L.; Ast, S.; Miao, H.; Chen, Y.; Schnabel, R. Beating the Standard Sensitivity-Bandwidth Limit of Cavity-Enhanced Interferometers with Internal Squeezed-Light Generation. *Phys. Rev. Lett.* **2017**, *118*, 143601. doi:10.1103/PhysRevLett.118.143601.
15. Zhao, Y.; Aritomi, N.; Capocasa, E.; Leonardi, M.; Eisenmann, M.; Guo, Y.; Polini, E.; Tomura, A.; Arai, K.; Aso, Y.; Huang, Y.C.; Lee, R.K.; Lück, H.; Miyakawa, O.; Prat, P.; Shoda, A.; Tacca, M.; Takahashi, R.; Vahlbruch, H.; Vardaro, M.; Wu, C.M.; Barsuglia, M.; Flaminio, R. Frequency-Dependent Squeezed Vacuum Source for Broadband Quantum Noise Reduction in Advanced Gravitational-Wave Detectors. *Phys. Rev. Lett.* **2020**, *124*, 171101. doi:10.1103/PhysRevLett.124.171101.
16. McCuller, L.; Whittle, C.; Ganapathy, D.; Komori, K.; Tse, M.; Fernandez-Galiana, A.; Barsotti, L.; Fritschel, P.; MacInnis, M.; Matichard, F.; Mason, K.; Mavalvala, N.; Mittleman, R.; Yu, H.; Zucker, M.E.; Evans, M. Frequency-Dependent Squeezing for Advanced LIGO. *Phys. Rev. Lett.* **2020**, *124*, 171102. doi:10.1103/PhysRevLett.124.171102.
17. Ackley, K.; Adya, V.B.; Agrawal, P.; Altin, P.; Ashton, G.; Bailes, M.; Baltinas, E.; Barbuio, A.; Beniwal, D.; Blair, C.; Blair, D.; Bolingbroke, G.N.; Bossilkov, V.; Boublil, S.S.; Brown, D.D.; Burridge, B.J.; Bustillo, J.C.; Cameron, J.; Cao, H.T.; Carlin, J.B.; Casey, A.; Chang, S.; Charlton, P.; Chatterjee, C.; Chattopadhyay, D.; Chen, X.; Chi, J.; Chow, J.; Chu, Q.; Ciobanu, A.; Clarke, T.; Clearwater, P.; Cooke, J.; Coward, D.; Crisp, H.; Dattatri, R.J.; Deller, A.T.; Dobie, D.A.; Dunn, L.; Easter, P.J.; Eichholz, J.; Evans, R.; Flynn, C.; Foran, G.; Forsyth, P.; Gai, Y.; Galaudage, S.; Galloway, D.K.; Gendre, B.; Goncharov, B.; Goode, S.; Gozzard, D.; Grace, B.; Graham, A.W.; Heger, A.; Vivanco, F.H.; Hirai, R.; Holland, N.A.; Holmes, Z.J.; Howard, E.; Howell, E.; Howitt, G.; Hübner, M.T.; Hurley, J.; Ingram, C.; Hamedan, V.J.; Jenner, K.; Ju, L.; Kapasi, D.P.; Kaur, T.; Kijbunchoo, N.; Kovalam, M.; Choudhary, R.K.; Lasky, P.D.; Lau, M.Y.M.; Leung, J.; Liu, J.; Loh, K.; Mailvagan, A.; Mandel, I.; McCann, J.J.; McClelland, D.E.; McKenzie, K.; McManus, D.; McRae, T.; Melatos, A.; Meyers, P.; Middleton, H.; Miles, M.T.; Millhouse, M.; Mong, Y.L.; Mueller, B.; Munch, J.; Musiov, J.; Muusse, S.; Nathan, R.S.; Naveh, Y.; Neijssel, C.; Neil, B.; Ng, S.W.S.; Oloworaran, V.; Ottaway, D.J.; Page, M.; Pan, J.; Pathak, M.; Payne, E.; Powell, J.; Pritchard, J.; Puckridge, E.; Raidani, A.; Rallabhandi, V.; Reardon, D.; Riley, J.A.; Roberts, L.; Romero-Shaw, I.M.; Roocke, T.J.; Rowell, G.; Sahu, N.; Sarin, N.; Sarre, L.; Sattari, H.; Schiworski, M.; Scott, S.M.; Sengar, R.; Shaddock, D.; Shannon, R.; SHI, J.; Sibley, P.; Slagmolen, B.J.J.; Slaven-Blair, T.; Smith, R.J.E.; Spollard, J.; Steed, L.; Strang, L.; Sun, H.; Sunderland, A.; Suvorova, S.; Talbot, C.; Thrane, E.; Töyrä, D.; Trahanas, P.; Vajpeyi, A.; van Heijningen, J.V.; Vargas, A.F.; Veitch, P.J.; Vigna-Gomez, A.; Wade, A.; Walker, K.; Wang, Z.; Ward, R.L.; Ward, K.; Webb, S.; Wen, L.; Wette, K.; Willcox, R.; Winterflood, J.; Wolf, C.; Wu, B.; Yap, M.J.; You, Z.; Yu, H.; Zhang, J.; Zhang, J.; Zhao, C.; Zhu, X. Neutron Star Extreme Matter Observatory: A kilohertz-band gravitational-wave detector in the global network, 2020, [arXiv:astro-ph.HE/2007.03128].
18. Rinkleff, R.H.; Wicht, A. The Concept of White Light Cavities Using Atomic Phase Coherence. *Physica Scripta* **2005**, p. 85. doi:10.1238/physica.topical.118a00085.
19. Miao, H.; Ma, Y.; Zhao, C.; Chen, Y. Enhancing the Bandwidth of Gravitational-Wave Detectors with Unstable Optomechanical Filters. *Phys. Rev. Lett.* **2015**, *115*, 211104. doi:10.1103/PhysRevLett.115.211104.
20. Page, M.A.; Goryachev, M.; Miao, H.; Chen, Y.; Ma, Y.; Mason, D.; Rossi, M.; Blair, C.D.; Ju, L.; Blair, D.G.; Schliesser, A.; Tobar, M.E.; Zhao, C. Gravitational wave detectors with broadband high frequency sensitivity, 2020, [arXiv:physics.optics/2007.08766].
21. Danilishin, S.L.; Khalili, F.Y.; Miao, H. Advanced quantum techniques for future gravitational-wave detectors. *Living Reviews in Relativity* **2019**, *22*, 2. doi:10.1007/s41114-019-0018-y.
22. Adhikari, R.X.; Arai, K.; Brooks, A.F.; Wipf, C.; Aguiar, O.; Altin, P.; Barr, B.; Barsotti, L.; Bassiri, R.; Bell, A.; Billingsley, G.; Birney, R.; Blair, D.; Bonilla, E.; Briggs, J.; Brown, D.D.; Byer, R.; Cao, H.; Constancio, M.; Cooper, S.; Corbitt, T.; Coyne, D.; Cumming, A.; Daw, E.; deRosa, R.; Eddolls, G.; Eichholz, J.; Evans, M.; Fejer, M.; Ferreira, E.C.; Freise, A.; Frolov, V.V.; Gras, S.; Green, A.; Grote, H.; Gustafson, E.; Hall, E.D.; Hammond, G.; Harms, J.; Harry, G.; Haughian, K.; Heinert, D.; Heintze, M.; Hellman, F.; Hennig, J.;

Hennig, M.; Hild, S.; Hough, J.; Johnson, W.; Kamai, B.; Kapasi, D.; Komori, K.; Koptsov, D.; Korobko, M.; Korth, W.Z.; Kuns, K.; Lantz, B.; Leavey, S.; Magana-Sandoval, F.; Mansell, G.; Markosyan, A.; Markowitz, A.; Martin, I.; Martin, R.; Martynov, D.; McClelland, D.E.; McGhee, G.; McRae, T.; Mills, J.; Mitrofanov, V.; Molina-Ruiz, M.; Mow-Lowry, C.; Munch, J.; Murray, P.; Ng, S.; Okada, M.A.; Ottaway, D.J.; Prokhorov, L.; Quetschke, V.; Reid, S.; Reitze, D.; Richardson, J.; Robie, R.; Romero-Shaw, I.; Route, R.; Rowan, S.; Schnabel, R.; Schneewind, M.; Seifert, F.; Shaddock, D.; Shapiro, B.; Shoemaker, D.; Silva, A.S.; Slagmolen, B.; Smith, J.; Smith, N.; Steinlechner, J.; Strain, K.; Taira, D.; Tait, S.; Tanner, D.; Tornasi, Z.; Torrie, C.; Veggel, M.V.; Vanheijningen, J.; Veitch, P.; Wade, A.; Wallace, G.; Ward, R.; Weiss, R.; Wessels, P.; Willke, B.; Yamamoto, H.; Yap, M.J.; Zhao, C. A cryogenic silicon interferometer for gravitational-wave detection. *Classical and Quantum Gravity* **2020**, *37*, 165003. doi:10.1088/1361-6382/ab9143.

23. The ET Science Team. *Einstein gravitational wave Telescope conceptual design*; European Commission, 2011.
24. ET Steering Committee Editorial Team. *Einstein Telescope design report update 2020*; Einstein Telescope Collaboration, 2020.
25. Abbott, B.P.; Abbott, R.; Abbott, T.D.; Abernathy, M.R.; Ackley, K.; Adams, C.; Addesso, P.; Adhikari, R.X.; others. Exploring the sensitivity of next generation gravitational wave detectors. *Classical and Quantum Gravity* **2017**, *34*, 044001. doi:10.1088/1361-6382/aa51f4.